Evaluation of Five Mammalian Models for Human Disease Research Using Genomic and Bioinformatic Approaches

Sankarasubramanian Jagadesan [#] , Pinaki Mondal [#] , Mark A Carlson , Chittibabu Guda [*]

Posted Date: 26 May 2023

doi: 10.20944/preprints202305.1816.v1

Keywords: Animal models; NHPs; rodents; marmoset; sequence similarity; SNPs; human diseases

Article

Evaluation of Five Mammalian Models for Human Disease Research Using Genomic and Bioinformatic Approaches

Sankarasubramanian Jagadesan [1,#], Pinaki Mondal [2#], Mark A Carlson [1,2] and Chittibabu Guda [1,3,*]

[1] Department of Genetics, Cell Biology, and Anatomy, University of Nebraska Medical Center, Omaha, NE 68198, USA email: s.jagadesan@unmc.edu; babu.guda@unmc.edu

[2] Department of Surgery and Center for Advanced Surgical Technology, University of Nebraska Medical Center, Omaha, NE 68198, USA email: pinaki.mondal@unmc.edu; macarlso@unmc.edu

[3] Center for Bioinformatics Research and Innovation, University of Nebraska Medical Center, Omaha, NE 68198, USA

* Correspondence : Chittibabu Guda, Ph.D. Professor & Vice Chair, Department of Genetics, Cell Biology, and Anatomy, University of Nebraska Medical Center, Omaha, NE 68198 USA. : email: babu.guda@unmc.edu; Tel.: +1 (402) 559-5954

[#] authors contributed equally

Abstract: The suitability of an animal model to study human diseases heavily relies on the similarity between the two species at the genetic, epigenetic, gene expression and metabolic levels. However, consistent data from different animal models at each level to evaluate this suitability is lacking. With the availability of genome sequences for many mammalian species it is now possible to compare animal models based on the genomic similarities. Here, we compare the coding sequences (CDS) of five mammalian models that include rhesus macaque, marmoset, pig, mouse and rat with those from human. We identified 10,316 conserved CDS across the five organisms and human based on the sequence similarity. Mapping the human disease-associated single nucleotide polymorphisms (SNPs) from these conserved CDS in each species has identified species-specific association with various human diseases. While associations for a disease such as colon cancer were prevalent in multiple model species, pig showed the highest number (117 diseases) of model-specific human disease associations. Based on the percentage of disease-associated SNP-containing genes, marmoset models are well suited to study many human ailments including behavioral and gastrointestinal diseases. Comparison of gene expression levels of the conserved CDS from colon, heart, kidney, lung, skeletal muscle, and spleen tissues in these models showed correlations with human expression levels in a tissue-specific manner. In the gastrointestinal tissues (colon, spleen), the pig showed the highest correlation while mouse displayed a better correlation in the heart and kidney. This study demonstrated genomic as well as tissue-specific expression-based similarity evaluation of five animal models against human that could help investigators select a suitable animal model to study their targeted disease.

Keywords: animal models; NHPs; rodents; marmoset; sequence similarity; SNPs; human diseases

1. Introduction

A comprehensive understanding of the genomic and gene expression relatedness between human and other mammals is necessary to evaluate the common pathways, functional similarities and appropriateness of different animal models to study human diseases. Although mouse is the most commonly used animal model to study human diseases [1], a smaller size and lifespan, and differences in the latency period for a disease [2] and drug metabolism [3], inflammatory response [4], and other processes [5–8] suggest, the need to identify larger animal models to study human diseases. Comparison of genomic sequences among human, mouse and pig indicated that pig sequences were closer to those of the human with more numbers of ultra-conserved regions

 doi:10.20944/preprints202305.1816.v1

compared to mouse [9–11]. The nonhuman primates are evolutionarily more closely related to human. After the ban on working with Chimpanzees and other great apes, macaques have become the most closely related nonhuman primate model to study human diseases [12]. Human disease genes and known drug domains have shown high degree of similarity with rhesus macaque genome [13]. The marmoset, on the other hand, is a useful animal model due to its short gestation and sexual maturation periods while having more sequence similarity with humans than rodents [12]. It is also a useful model to studying diseases in neurobiology [14]. A comparative analysis of gene expression and disease-associated genetic variations across commonly used animal models will help understand the similarities leading to appropriate use of specific animal models for disease-specific research.

In this study, we retrieved the protein-coding sequences (CDS) from two rodents (mouse and rat), the pig, two nonhuman primates (rhesus macaque and marmoset) and humans to identify conserved CDS across the six species. Single nucleotide polymorphisms (SNPs) from these CDS were mapped to corresponding disease associations to identify common and unique clinically associated SNPs to better define the relevance of an animal model with various human diseases. Finally, comparative transcriptomic analysis of different tissues was performed for conserved CDS in human, mouse and pig (data from marmoset and rhesus macaque were not available) to identify common tissue-specific expression profiles of the conserved CDS to identify the disease-specific relevance of these animal models.

2. Materials and Methods

2.1. Retrieval of protein-coding sequences

Genomic data for human, rhesus macaque, pig, mouse and rat were retrieved from Ensembl [15] and for marmoset from National Center for Biotechnology Information (NCBI). Datasets include *Homo sapiens* (Human - GCA_000001405.28), *Macaca mulatta* (Rhesus macaque - GCA_003339765.3), *Callithrix jacchus* (Marmoset – NCBI: GCF_009663435.1), *Sus scrofa* (Pig - GCA_000003025.6), *Mus musculus* (Mouse - GCA_000001635.9) and *Rattus norvegicus* (Rat - GCA_000001895.4). We have extracted a total of 19,962 human, 21,591 rhesus macaque, 22,252 marmoset, 21,280 pig, 21,848 mouse and 22,250 rat coding sequences (CDS) for current analysis.

2.2. Identification of similarity between human CDS and other mammalian sequences

Five pairwise sequence comparisons were performed to identify the conserved human CDS that include human vs. rhesus macaque, human vs. marmoset, human vs. pig, human vs. mouse, and human vs. rat. The Basic Local Alignment Search Tool (BLAST) would align and compare a query DNA sequence with a database of sequences. The BLAST database was constructed for human sequences using the makeblastdb application. CDS from the rhesus macaque, marmoset, pig, mouse, and rat sequences were queried against the human BLAST database using BLASTn (options: -max_hsps 1 -max_target_seqs 1) in BLAST+ (version 2.7.1) [16]. Based on the pairwise alignment, we identified conserved CDS for other mammals against the human. Some sequences from blast hits showed low coverage. To avoid the false positives, we filtered the sequences with greater than 50% identity and covered at least 50% length of the human CDS. Alignments that fall below these criteria were excluded for further analysis. Based on these similarities, conserved sequences were identified across the five comparisons and plotted using UpSetR [17]. To understand the synteny block distribution for the human conserved CDS on different chromosomes of the five species, we created circos plots using the R package, shinyCircus [18] using the human chromosome as the reference.

2.3. Comparison of conserved CDS and identification of SNPs and their associated diseases

Multiple sequence alignment was performed across the six species using 10,316 conserved CDS using ClustalW2 [19]and SNPs were extracted from the alignment using SNP-sites [20] and msa2snp (https://github.com/pinbo/msa2snp). The Ensembl Variant Effect Predictor [21] was used to identify SNPs with rs ID (RefSeq) Later, Ensembl Post GWAS and SNPnexus (uses Cosmic, ClinVar and GWAS) [22] were used to predict human SNP-associated diseases. These diseases were further

Preprints (www.preprints.org) | NOT PEER-REVIEWED | Posted: 26 May 2023 doi:10.20944/preprints202305.1816.v1

classified under 25 different categories using the DisGeNET [23]. Further, we have calculated the percentage for each disease category (Number of diseases in each category / Total number of identified diseases) across all the comparisons. We also identified the conserved and species-specific SNPs associated with disease for a particular animal model. Those SNPs were plotted using R packages, such as shinyCircus [18] and karyoploteR [24].

2.4. Construction of phylogenetic tree

Multiple sequence alignments of 10,316 conserved CDS from six organisms were concatenated as per their order on the human chromosome (1-22, X and Y) using EMBOSS Union [25]. The phylogeny was constructed using FastTree (parameter –nt –gtr) version 2.1 [26] and visualized using Molecular Evolutionary Genetics Analysis (MEGA) version 11 [27].

2.5. Transcriptomic analysis using tissue-specific data

We retrieved RNA-seq expression data on six tissues (colon, heart, kidney, lung, skeletal muscle and spleen) for human, mouse, rat and pig from the Expression Atlas database [28] with a default minimum expression value of 0.5 Transcripts Per Million (TPM). Such data for marmoset and rhesus macaque were not available, hence these two species were excluded from the transcriptomic analysis. Conserved genes based on our aforementioned BLAST analysis for each tissue were filtered for the four organisms. Correlation analysis was carried out using the R package, corrplot [29] to detect tissues with highly similar gene expression profiles between the model organisms and the human. Pearson correlation coefficient was used to measure the linear dependence between two variables.

3. Results

3.1. Identification of conserved CDS with human sequences

We compared the coding sequences between human and five other species using the BLAST program with cutoffs of at least 50% sequence identity and 50% length match to the human sequences. Results showed that rhesus macaque has the highest average identity (96.82%) followed by marmoset (94.65%), pig (89.37%), mouse (86.65%) and rat (86.53%) (Table 1). The percent identity ranged from 100 to around 70 that is comparable across all comparison groups (Table 1). However, the distribution of percent identity of the CDS is not uniform in all comparison groups. In rhesus macaque and marmoset, the identity distribution is skewed towards the median (median for rhesus macaque is: 97.29 and for marmoset is 95.29, Supplementary Table S1), denoting that the majority of the CDS in these primate species are highly identical to human CDS (Figure 1a). On the other hand, the identities in pig, mouse and rat are more widely distributed around the median suggesting a varying degree of similarity with certain gene families of human (Figure 1a and Supplementary Table S1). Among these three organisms, pigs showed the highest median value (89.89% identity) and significantly higher percent identity with human CDS than those of mouse or rat (Figure 1a). The complete result of this identity analysis is provided in Supplementary Table S2.

Table 1. Comparison of sequence identity among the CDS between human and five other mammalian animal models.

Comparison	Identified Blast hits*	Average percentage identity	Range of percent identity	Average percentage identity for conserved CDS
Human vs. Rhesus macaque	17,638	96.82	100-71.74	97.53
Human vs. Marmoset	17,787	94.65	100-71.63	95.76
Human vs. Pig	14,992	89.37	100-70.81	90.38
Human vs. Mouse	13,806	86.65	100-70.11	87.19
Human vs. Rat	13,222	86.53	100-68.93	87.04

* At least 50% sequence identity and 50% or higher length match to human CDS.

Preprints (www.preprints.org) | NOT PEER-REVIEWED | Posted: 26 May 2023 doi:10.20944/preprints202305.1816.v1

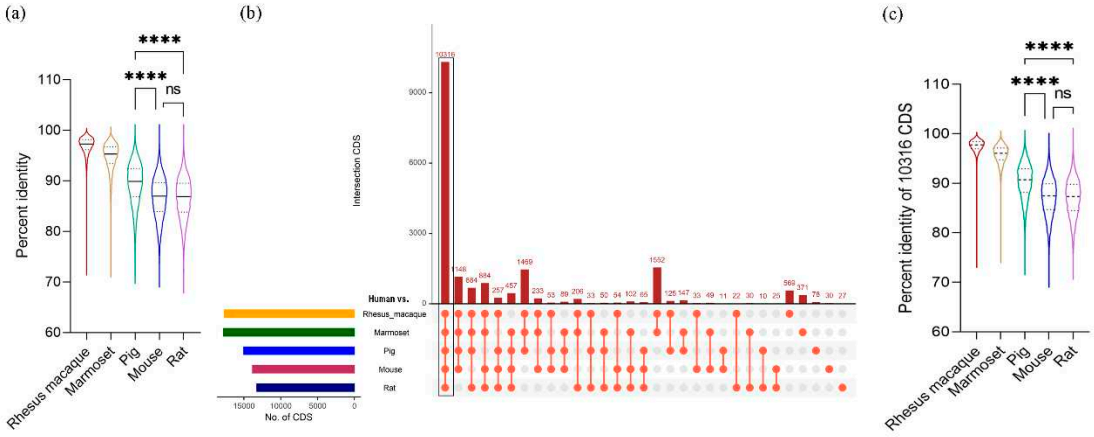

Figure 1. Similarity of coding sequences (CDS) between human and animal models. a) Distribution of the CDS identity percentages with human in five different models. The line inside the violin plot represents median values. b) The total number of mapped CDS in five different species against human. The upset plot shows intersections across the five comparisons. Each bar represents the number of mapped CDS and the orange dot below the bar indicates their conservation status across each species. c) Distribution of percentage identities of 10,316 conserved CDs between human and five animal models. The line inside the violin plot represents median values. **** denotes p-value <0.0001, ns = statistically non-significant as determined by Kruskal-Wallis non-parametric test.

Based on the pairwise alignment of CDS between human and five other species, 10,316 CDS were found to be conserved across all six species (Figure 1b and Supplementary Table S2), which were used for further analyses. In all species, these conserved set of CDS recorded higher percentage identities than those involving all CDS (Table 1). Among the non-human primates, rhesus macaque showed the highest average identity with the human at 97.53% and pigs showed 90.38% identity, which is significantly higher than those of mice and rats (Figure 1c and Supplementary Table S3).

Next, we mapped all conserved CDS from each non-human species to matching positions (by similarity) on human chromosomes to understand their synteny distribution in each species. For this purpose, we used a common color-coding scheme for each chromosome number where the same color represents the same chromosome number in all species. Of note, marmoset has the same number of chromosomes as the human but the other species have fewer. Pig has the least number of with only 18 chromosomes. The circos plots (Figure 2a) illustrate the mapping of synteny blocks (represented by CDS) from different chromosomes of non-human species using the human chromosomal numbers as a reference. The chromosomes in the non-human species mapped with only color indicate that they contain corresponding human synteny blocks intact and those showing mosaic coloring indicate that the human synteny blocks are distributed on different chromosomes as indicated by different colors. For instance, synteny blocks of conserved CDS from chromosome 1 of macaque (shown in red color) also map to chromosome 1 of the human, but corresponding synteny blocks from other species are mapped to different human chromosomal locations. Similarly, synteny blocks from chromosomes 12 and 13 of the macaque are mapped to chromosome 2 of the human. Of note, the synteny blocks on chromosomes 17, 20 and X are intact in a single chromosome in all the species (as indicated by only one color) while those from other chromosomes are fragmented and distributed in multiple chromosomes (with mosaic color mapping) (Table 2).

Preprints (www.preprints.org) | NOT PEER-REVIEWED | Posted: 26 May 2023 doi:10.20944/preprints202305.1816.v1

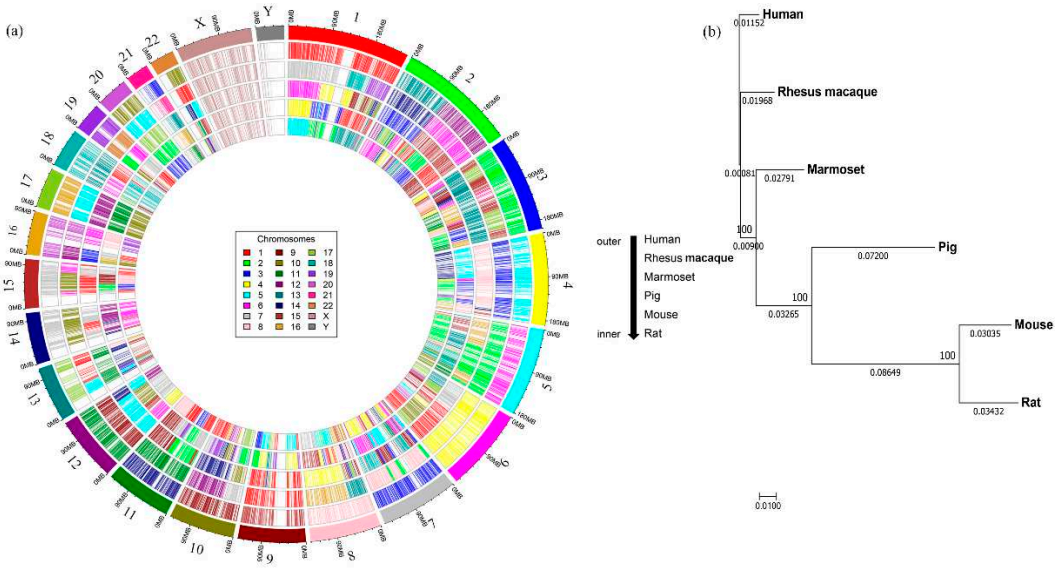

Figure 2. Mapping of the synteny blocks of model organism chromosomes on to the human chromosomes and phylogenetic analysis. a) The Circos plot shows the position of 10,316 conserved CDS for five different animal models using a unique color for each chromosome number. The outermost circle represents the color-coded human chromosomes and each inner circle represents mapping of the synteny blocks of chromosomes from each species on to the human chromosomes showing how they are distributed across the human chromosomes. The chromosome numbers vary across each species with rhesus macaque containing Chr1-20, X, Y; marmoset with Chr1-22, X, Y; pig (Chr1-18, X, Y); mouse (Chr1-21, X, Y); and rat (Chr1-20, X, Y). b) A phylogenetic tree was constructed based on the 10,316 conserved CDS, which showed that the evolutionary distance with human was closest for rhesus macaque, followed by marmoset, pig, mouse and rat. The values above and below the line indicate the bootstrap numbers and evolutionary distance between the species.

Table 2. Chromosome-specific mapping of conserved CDS between human and animal model genomes.

Human Chromosomes	Total CDS	Conserved CDS	Rhesus macaque*	Marmoset*	Pig*	Mouse*	Rat*
Chr1	2049	1088	1	7, 18, 19	6, 4, 9, 10, 14, 2, 7	4, 3, 1, 8	5, 2, 13,19, 14, 10, 17, 4
Chr2	1244	750	12, 13	6, 14	15, 3	1, 2, 6, 17, 12, 11	9, 6, 3, 4, 14, 13, 20, 18
Chr3	1075	645	2	15, 17	13	9, 16, 3, 6, 14	8, 11, 2, 4, 16, 15
Chr4	752	390	5	3	8, 15, 14	5, 3, 8	14, 2, 16, 19, 4
Chr5	883	502	6	2	2, 16	13, 18, 11, 15	2, 18, 10, 17, 1, 9
Chr6	1045	574	4	4	7, 1	17, 10, 13, 9, 4, 1	20, 1, 17, 9, 8, 5
Chr7	919	470	3	8,2	18, 9, 3	5, 6, 12, 11, 13	4, 12, 6, 14, 17
Chr8	684	372	8	16, 13	4, 14,17, 15	15, 8, 14, 4, 1, 3	7, 5, 16, 15, 2, 11
Chr9	779	402	15	1	1, 10, 14 3	4, 2, 19, 13	5, 3, 1, 17
Chr10	1309	619	9	12, 7	14, 10	19, 14, 2, 10, 7, 18, 6, 13	1, 17, 20, 16, 15, 4
Chr11	727	432	14	11	2, 9	7, 9, 19, 2	1, 8, 3
Chr12	1033	582	11	9	5, 14	10, 5, 6, 15	7, 12, 4
Chr13	321	182	17	1, 5	11	14, 8, 5, 3	15, 16, 12, 2, 9
Chr14	610	360	7	10	7, 1	12, 14	6, 15
Chr15	596	371	7	10, 6	1, 7	9, 2, 7	8, 3, 1
Chr16	851	378	20	12, 20	6, 3	8, 7, 16, 17, 11	19, 1, 10
Chr17	1182	637	16	5	12	11	10
Chr18	269	157	18	13	1, 6	18, 17, 1	18, 9, 3

Preprints (www.preprints.org) | NOT PEER-REVIEWED | Posted: 26 May 2023 doi:10.20944/preprints202305.1816.v1

Chr19	546	282	19	22	6, 2	7, 8, 10, 17, 9	1, 7, 16, 8, 19, 9, 12
Chr20	1469	457	10	5	17	2	3
Chr21	234	76	3	21	13	16, 10, 17	11, 20
Chr22	444	202	10	1	5, 14	15, 11, 16, 5, 10	7, 14, 11, 12, 20
ChrX	853	381	X	X	X	X	X
ChrY	46	7	Y	Y, X	Y, X	Y, X	Y, X

* Chromosome numbers are listed according to the highest to lowest number of CDS mapped to the human.

Phylogenetic analysis based on conserved CDS examines the evolutionary distances among the six species. As shown in Figure 2b, the nonhuman primate (NHP) group has the closest distance to human with the pig positioned in the middle and the rodent group being the farthest from the human. The chromosome specific mapping for all the CDS and conserved CDS were presented in Supplementary Table S4 and S5, respectively.

3.2. Mapping human disease-relevant SNPs in other species

Mapping of human SNPs to the other species after multiple sequence alignment of 10,316 conserved CDS showed differences in the SNP numbers between the primates and other three organisms. Primates had lower number of predicted SNPs (rhesus macaque: 63,449 and marmoset: 40,181) in the conserved CDS than pig (145,715), mouse (221,383) and rat (220,630). A full list of all the SNPs is provided in the Supplementary Table S6. The SNPs were then annotated for disease association. Even with a very low number of human SNPs mapped, comparable number of disease associations were identified in rhesus macaque and marmoset as in other three animals (Table 3). The disease-associated SNPs in each of these six organisms were plotted on each chromosome to easily visualize the distribution and variation of the SNPs across species (Supplementary Figure S1). The identified diseases with their corresponding rs ID for human versus five animals were listed in Supplementary Table S7 and Supplementary Figure S2–S6. Among the predicted diseases based on the human SNPs, 772 were conserved among all six species (Figure 3a). These 772 diseases were then classified into tissue-specific diseases and compared amongst the five non-human model organisms based on the disease prediction score. The higher the score, the more relevance to the human diseases. Congenital, hereditary and neonatal diseases and abnormalities and nervous system diseases were highly prevalent in all the models (Figure 3b), while some disease classes were specific to a model organism. SNPs associated with reproductive system diseases were specifically observed in rhesus macaque; behavioral and gastrointestinal diseases in marmoset; cancer and metabolic diseases in pigs; and hepatic and cardiovascular diseases are prevalent in rats and mice (Figure 3b). These results indicate that human SNPs associated with specific disease classes are prevalent in specific model species, which may provide a basis for selection of appropriate model for a specific disease.

Table 3. Number of human SNPs mapped to the conserved CDS across five animal models and their associated disease information.

Organisms	Total SNPs in 10,316 CDS with RS number	SNPs associated with disease	SNPs identified in genes	No. of identified diseases	Species-specific diseases*
Human vs. Rhesus macaque	63,449	2198	1074	1255	77 (77)
Human vs. Marmoset	40,181	1533	867	1039	4 (12)
Human vs. Pig	145,715	4011	1428	1597	117 (96)
Human vs. Mouse	221,383	5824	1630	1798	58 (44)
Human vs. Rat	220,631	5739	1646	1787	81 (54)

* Number inside the brackets indicates the number of genes

Preprints (www.preprints.org) | NOT PEER-REVIEWED | Posted: 26 May 2023 doi:10.20944/preprints202305.1816.v1

(a)

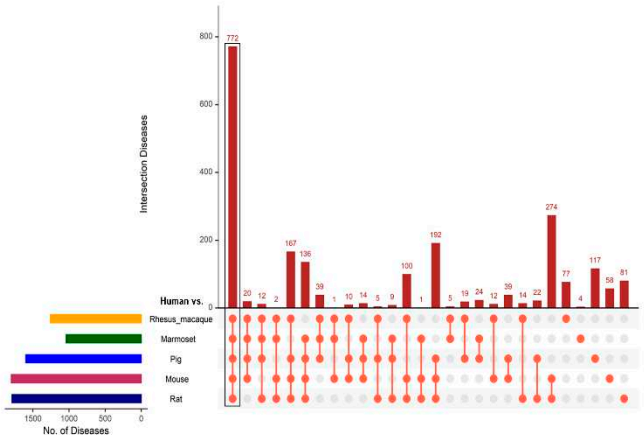

(b)

Disease class name	Rhesus macaque	Marmoset	Pig	Mouse	Rat
Chemically-Induced Disorders	0.05	0.02	0.03	0.01	0.01
Endocrine System Diseases	1.96	1.85	1.67	1.46	1.46
Eye Diseases	3.33	3.14	3.24	3.31	3.32
Hematological Diseases	2.98	2.56	2.69	2.57	2.41
Immune System Diseases	1.33	1.16	1.03	1.01	0.91
Male Urogenital Diseases	2.48	2.26	2.13	2.23	2.20
Otorhinolaryngologic Diseases	1.56	1.25	1.41	1.47	1.48
Pathological Conditions, Signs and Symptoms	5.64	5.08	5.13	5.33	5.51
Reproductive System Diseases	2.86	2.54	2.47	2.58	2.53
Behavior and Behavior Mechanisms	2.21	2.93	1.97	1.76	1.70
Gastrointestinal Diseases	2.09	2.54	2.31	2.17	2.14
Infections	0.17	0.22	0.19	0.14	0.18
Other Diseases	17.20	18.51	16.93	15.88	15.86
Cancer	5.11	5.66	6.06	5.92	5.94
Dermatological Diseases and Conditions	3.85	3.72	3.99	3.70	3.62
Nutritional and Metabolic Diseases	5.74	6.13	6.16	5.68	5.88
Organismal Injury and Abnormalities	1.69	1.98	2.01	1.93	1.95
Congenital, Hereditary, and Neonatal Diseases and Abnormalities	16.96	16.68	17.93	18.08	18.04
Respiratory Diseases	0.91	0.93	0.75	0.95	0.93
Cardiovascular Diseases	5.83	5.19	5.63	6.14	6.14
Stomatognathic Diseases	0.42	0.43	0.42	0.46	0.46
Musculoskeletal Diseases	5.14	4.63	5.12	5.84	5.88
Nervous System Diseases	10.44	10.48	10.67	11.28	11.33
Hepatic System Diseases	0.06	0.11	0.08	0.10	0.11

Figure 3. Comparison of the SNPs associated human diseases across the animal models. a) An upset plot shows the intersections of SNP-associated human diseases across the five species. Each bar represents the number of identified diseases and the orange dot below the bar indicates their conservation across the comparisons. b) The diseases were classified into 25 different categories and the percentages of a specific disease class in each animal model were plotted. Higher to lower percentage numbers within species are colored from green to yellow. The highest value across species for each disease class is indicated by a box.

Next, we investigated any model-specific SNP association with human diseases. The pig had the highest number; 117 diseases from 96 SNPs were specific to pigs (Table 3). The marmoset had the lowest number with only four diseases specifically associated with this species. We have provided a curated list of all model-specific human-associated diseases and identified SNPs with their corresponding genes (Supplementary Table S8). In our study, none of the disorders were noted in chromosome Y. The pig model had a wide range of distinct diseases spread across all the chromosomes. Exclusively, the two genes detected in chromosome 13, COG6 and EDNRB associated with the pig model cause Shaheen syndrome and Hirschsprung disease (Figure 4).

Preprints (www.preprints.org) | NOT PEER-REVIEWED | Posted: 26 May 2023 doi:10.20944/preprints202305.1816.v1

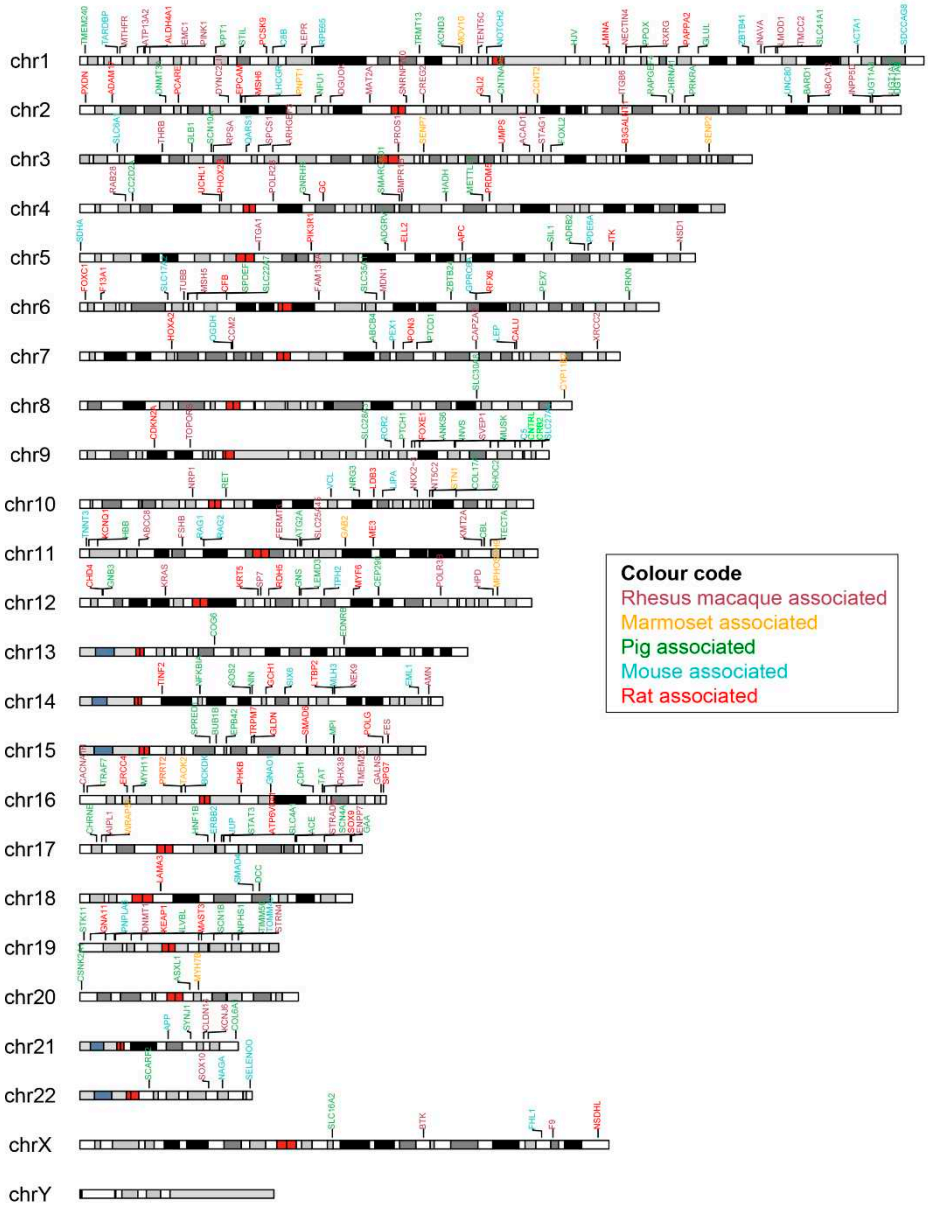

Figure 4. Mapping of human SNP-associated genes in different animal models across the human chromosomes. The identified SNPs associated genes for species-specific diseases were represented with different colors using Karyoplot.

Next, we identified the human SNP-bearing genes in the animal models that showed an association with a human disease as shown in the color-coded chromosomal map (Figure 4). The genes that showed the highest number of disease associations in each animal model corresponding to each human chromosome were listed in Table 4. The full list of genes per chromosome is provided in Supplementary Table S7. Six common genes (ATM, POLE, RB1, FBN1, TSC2 and FLNA) were identified across species which were the topmost genes associated with the highest number of diseases in different chromosomes. Two DNA mismatch repair proteins, MSH6 in human chromosome 2 and MLH1 in chromosome 3 were found to have very high disease-association across pig, mouse and rat models. SNPs associated with the Chromosome 7 encoded CFTR (cystic fibrosis transmembrane conductance regulator) gene were high associated in rat and mouse models but not so much in other species. Another gene, PTCH1 (protein patched homolog 1) that is a component of hedgehog pathway is associated with a number of diseases in pigs, especially Holoprosencephaly 7, was identified only in the pig model.

Preprints (www.preprints.org) | NOT PEER-REVIEWED | Posted: 26 May 2023 doi:10.20944/preprints202305.1816.v1

Table 4. Genes in each species that are identified with the highest number of human diseases in each human chromosome.

Chromosome	Rat*	Diseases	Mouse*	Diseases	Pig*	Diseases	Marmoset*	Diseases	Rhesus macaque*	Diseases
1	*ABCA4*	41	*MUTYH*	44	*SPTA1*	34	*NLRP3*	15	*SPTA1*	18
2	*MSH6*	115	*MSH6*	97	*MSH6*	78	*APOB*	22	*APOB*	31
3	*MLH1*	36	*BAP1*	34	*MLH1*	34	*ITIH3*	21	*ITIH3*	21
4	*WFS1*	23	*PDGFRA*	27	*KIT*	29	*KIT*	13	*PDGFRA*	18
5	*SDHA*	55	*SDHA*	75	*SDHA*	35	*VCAN*	21	*SDHA*	14
6	*DSP*	40	*DSP*	52	*SLC22A7*	12	*CFB*	6	*DSP*	28
7	*CFTR*	39	*CFTR*	38	*GARS1*	19	*GARS1*	13	*RELN*	14
8	*NBN*	17	*NBN*	17	*NBN*	23	*KCNQ3*	7	*FGFR1*	7
9	*NOTCH1*	95	*NOTCH1*	102	*PTCH1*	55	*COL5A1*	13	*NOTCH1*	25
10	*RET*	57	*RET*	55	*RET*	65	*RET*	25	*CUBN*	14
11	*ATM*	125	*ATM*	117	*ATM*	116	*ATM*	43	*ATM*	37
12	*POLE*	107	*POLE*	118	*POLE*	78	*POLE*	24	*POLE*	24
13	*RB1*	15	*RB1*	14	*RB1*	8	*RB1*	5	*RB1*	8
14	*DYNC1H1*	43	*DYNC1H1*	44	*DICER1*	24	*C14orf39*	8	*DICER1*	10
15	*FBN1*	140	*FBN1*	152	*FBN1*	120	*FBN1*	41	*FBN1*	36
16	*TSC2*	209	*TSC2*	215	*TSC2*	112	*TSC2*	38	*TSC2*	46
17	*SCN4A*	53	*SCN4A*	58	*NF1*	33	*AC004223.3*	17	*AC004223.3*	21
18	*LAMA3*	13	*LOXHD1*	15	*LAMA3*	14	*LAMA3*	4	*LOXHD1*	6
19	*LDLR*	72	*STK11*	59	*LDLR*	56	*LDLR*	22	*LDLR*	25
20	*COL9A3*	15	*SLC2A10*	18	*JAG1*	11	*MYH7B*	9	*MYH7B*	9
21	*COL6A1*	19	*COL6A1*	19	*CBS*	13	*CBS*	4	*CBS*	13
22	*NF2*	18	*DEPDC5*	17	*TMPRSS6*	29	*TMPRSS6*	26	*TMPRSS6*	28
X	*FLNA*	110	*FLNA*	118	*FLNA*	30	*FLNA*	14	*FLNA*	26

* Genes associate with human diseases

3.3. Transcriptomic analysis of six different tissues

To understand the gene expression similarities between human and the animal models, tissue-specific expression data were accessed from the Expression Atlas database [28]. Rhesus macaque and marmoset were excluded from the analysis due to non-availability of expression data. Colon, heart, kidney, lung, skeletal muscle and spleen were selected to examine the expression across species. The number of expressed genes in each tissue for the four organisms were identified and listed in Table 5. Gene expression corresponding to the 10,316 conserved CDS identified from the genomic analysis were taken from each tissue (Table 5) and used in subsequent analyses. When we examined the level of gene expression in each tissue and performed correlation analysis with each species, we found that gene expression in spleen of humans was most correlated with the pig followed by rat (Figure 5). The pig had the highest gene expression correlation with human in the lung and colon, while mouse had the highest in heart, kidney and skeletal muscle (Figure 5). The gene-level expression for four different organisms in six tissues was plotted in the heatmap and presented in Supplementary Figure S7–S12.

Table 5. List of expressed genes in various tissues and their conservation in human, mouse, rat and pig.

Tissues	Expressed genes				Conserved genes in four organisms based on 10316 CDS
	Human	Mouse	Rat	Pig	
Spleen	10,873	9,984	16,697	17,647	4,121
Skeletal muscle	10,590	10,650	12,770	15,152	3,963
Lung	11,285	11,213	18,171	12,943	4,034
Colon	11,125	10,755	16,949	15,603	4,128
Heart	10,967	10,369	14,821	13,995	4,116
Kidney	11,325	10,706	16,400	16,410	4,401

Preprints (www.preprints.org) | NOT PEER-REVIEWED | Posted: 26 May 2023 doi:10.20944/preprints202305.1816.v1

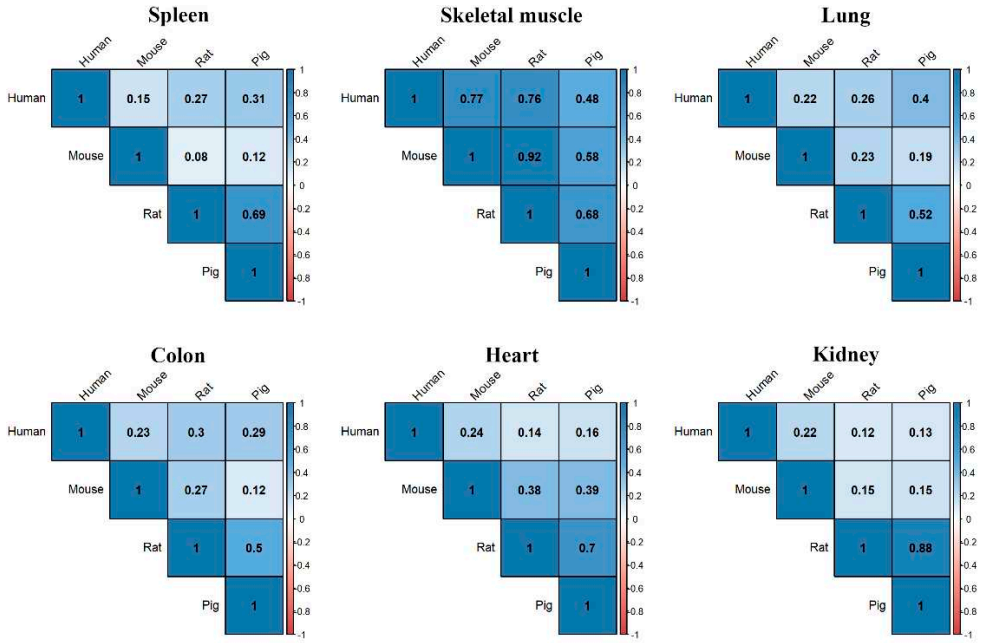

Figure 5. Correlation of tissue specific expression across different species. Correlation plot shows the similarity in tissue specific expression between human and other species. The correlation scale ranges from -1 to +1 and all values are in the positive range as indicated by the color.

4. Discussion

The selection of an animal models to study human diseases is based in part on the genetic relatedness to humans. However, species evolution is generally not synchronous with gene evolution, which results in certain human genes having more similarity in certain model organisms, which can influence the selection of different animal models for different research projects. Although primates are known to be evolutionary closer to human and can better mimic the human physiology, use of NHPs is expensive, time-consuming, heavily regulated, and subject to availability [30,31]. In this study, we have identified genetic similarity of CDS and mapped disease-associated human SNPs with commonly used animal models, the including the rhesus macaque, marmoset, pig, mouse, and the rat. We also compared human gene expression similarities in multiple tissue types in pig, rat and mouse.

Identification of NHPs as the closest evolutionary neighbors with the human was expected. BLAST-based genome-wide sequence comparison of rhesus macaque and marmoset with the human showed a 95-97% similarity across about 18,000 sequences, and the CDS-level identities also registered 96-98% similarity in these NHP models further supporting the belief that the macaque and marmoset are good animal models to study human diseases (Table 1). Alternatively, the pig's genome-level similarity (89.4%) with that of human was higher than that of the rat (86.7%) or mouse (86.5%). This observation remained true at the CDS-level, suggesting that pig is a more suitable model (with respect to genomics) to study human diseases than rodent models (Table 1).

It should also be noted that pig share the highest number of common genes (96) containing disease-associated SNPs with human than the other examined species (Table 3), which favors the pig model to study genetically predisposed human diseases. Similarly, these common SNPs between pig and human are also associated with the highest number of human diseases (117), further emphasizing the pig's strong relatedness to humans. We mapped the SNP- associated diseases on to different disease groups and observed that cancer-associated SNPs had the greatest number in pig; however, the difference in cancer mapping among species was not statistically significant. Nevertheless, examination of multiple levels of relatedness between humans and the pig (genome, CDS, SNPs and

 doi:10.20944/preprints202305.1816.v1

cancer disease levels) suggested that pig would be a more accurate genetic model for human cancer research than rodents.

SNP-associated behavioral diseases were mostly observed in the marmoset, which is in concordance with the existing literature [32,33]. Our analysis also suggested that the marmoset could also be used to model gastrointestinal diseases, which are found in the marmosets in captivity [34,35]. Endocrine and reproductive system diseases were found to be frequent in rhesus macaques, which contributes to the existing evidence supporting the use of the NHP model for adrenal androgen-related and endocrine-based social and reproductive studies [36,37]. Nutritional and metabolic disease-associated SNPs were also found to be high in pig. Pigs with high-caloric food intake are prone to developing metabolic syndrome [38,39]. In addition, the large body size, omnivorous diet and large gastrointestinal tract in pigs make them a suitable model for nutritional and pharmacological studies [39]. On the other hand, rodents showed a higher number of SNPs associated with musculoskeletal, cardiovascular and nervous system diseases. Rodents, specifically the rat have been used as hindlimb model to study musculoskeletal parameters [40]. A rat model for musculoskeletal implant infection was also developed recently [41]. The mouse has been widely used to study human heart diseases, mainly for myocardial infarction, heart fibrosis, and the cardiomyopathies [42–45]. Neurological disorders have also been studied using the rodent models, extensively [46,47].

When we specifically analyzed the chromosomes and genes which are associated with human diseases, prevalence of genes in the DNA repair pathway were most commonly found in all of the species. PTCH1 was the topmost SNP-prevalent gene in chromosome 9 for pigs. PTCH1 altered in 2.76% of all cancers was mostly observed to be altered in the colon cancer (TCGA data portal, My cancer genome database [48]. Similarly in mouse, STK11 was most commonly found in lung cancer appeared as the topmost gene in chromosome 19. Our tissue-based expression analysis also shed more light into the gene expression similarities with human for each species. In pigs, the spleen has the greatest number of genes commonly expressed with human, while the mouse had the lowest among the three species compared. Similarly, the rats had the higher numbers of expressed genes in lung, heart and colon, indicating an advantage of using the rat model for cardiovascular and colonic diseases. With the list of the genes presented in Table 4, suitable gene-based animal models could be considered to study different human diseases.

5. Conclusions

Using the whole genomic and coding sequence similarities, mapping the human SNPs on to the genomes of five other mammalian species, and tissue-specific expression analysis, this study demonstrated potentially important similarities and differences in genomics and transcriptomics among major model organisms with respect to humans. With respect to this analysis of sequence and expressional data, some species (e.g., NPHs) appeared to be more superior as models of human disease than other species. Overall, it was determined that the pig had greater sequence and expressional homology with humans than rodents had with humans. Based on these data, the pig emerged as a reasonable model to study human diseases, most notably cancer where a related immune system is present. Marmoset models are well positioned to study behavioral and gastrointestinal diseases. Rodents could be a better model for cardiovascular diseases, but have an obvious size discrepancy with humans, and have less overall sequence and expressional homology with humans than the pig has with humans. This study represents the suitability assessment based on the available genomic and expression data only; however, other factors such as cost, feasibility, and individual project goals should be carefully considered in selecting appropriate animal model for each research project.

Supplementary Materials: The following supporting information can be downloaded at the website of this paper posted on Preprints.org, **Table S1**, title: Distribution analysis of all CDS comparison between human and other species; **Table S2**, title: The predicted blast hits for human vs. rhesus macaque, marmoset, pig, mouse, and rat and the conserved 10,316 CDS were provided in each sheet; **Table S3**, title: Distribution analysis of 10,316 commons CDS comparison between human and other species; **Table S4**, title: Human CDS identified across the

rhesus macaque, marmoset, pig, mouse, and rat chromosomes were listed; **Table S5**, title: Identified 10316 conserved human CDS mapped across the rhesus macaque, marmoset, pig, mouse, and rat chromosomes were listed; **Table S6**, title: List of predicted SNPs with Refseq (RS) ID in 10,316 CDS in human vs. rhesus macaque, marmoset, pig, mouse, and rat using Ensembl Variant Effect Predictor; **Table S7**, title: Identified diseases from human vs. rhesus macaque, marmoset, pig, mouse, and rat using Ensembl Post GWAS and SNPnexus; **Table S8**, title: Human-associated specific diseases in rhesus macaque, marmoset, pig, mouse, and rat with their corresponding genes were listed; **Figure S1**, title: The number of disease-associated SNPs were plotted in a circus plot. The coloured circle differentiated the six different organisms (outer – inner: human, rhesus macaque, marmoset, pig, mouse, and rat), and the red line inside each circle represents the disease-associated SNPs; **Figure S2**, title: The number of identified diseases (orange) with their corresponding RefSeq (RS) ID (green), 1255 Variant−Disease Network, was provided for human vs. rhesus macaque; **Figure S3**, title: The number of identified diseases (orange) with their corresponding RefSeq (RS) ID (green), 1039 Variant−Disease Network, was provided for human vs. marmoset; **Figure S4**, title: The number of identified diseases (orange) with their corresponding RefSeq (RS) ID (green), 1597 Variant−Disease Network, was provided for human vs. pig; **Figure S5**, title: The number of identified diseases (orange) with their corresponding RefSeq (RS) ID (green), 1798 Variant−Disease Network, was provided for human vs. mouse; **Figure S6**, title: The number of identified diseases (orange) with their corresponding RefSeq (RS) ID (green), 1787 Variant−Disease Network, was provided for human vs. rat; **Figure S7**, title: Heatmap represents the number of expressed genes in spleen tissues across human, mouse, pig and rat; **Figure S8**, title: Heatmap represents the number of expressed genes in skeletal muscle tissues across human, mouse, pig and rat; **Figure S9**, title: Heatmap represents the number of expressed genes in lung tissues across human, mouse, pig and rat; **Figure S10**, title: Heatmap represents the number of expressed genes in colon tissues across human, mouse, pig and rat; **Figure S11**, title: Heatmap represents the number of expressed genes in heart tissues across human, mouse, pig and rat; **Figure S12**, title: Heatmap represents the number of expressed genes in kidney tissues across human, mouse, pig and rat.

Author Contributions: Conceptualization, C.G. and M.A.C.; methodology, S.J. and P.M.; software, S.J.; validation, P.M.; formal analysis, X.X.; investigation, C.G. and M.A.C.; resources, B.G.; data curation, S.J.; writing—original draft preparation, S.J. and P.M.; writing—review and editing, C.G and M.A.C.; visualization, S.J.; supervision, C.G. and M.A.C.; project administration, C.G.; funding acquisition, C.G. All authors have read and agreed to the published version of the manuscript.

Funding: This project was partly supported by NIH awards, 5R01CA222907 and 5R01AG062198 to MAC, and 5P20GM103427, 5P30CA036727, 2U54GM115458 to CG; and the Nebraska Research Initiative (NRI) to CG.

Acknowledgments: Authors would like to thank the Bioinformatics and Systems Biology Core (BSBC) facility at UNMC for providing the computational infrastructure and support. BSBC is partly supported by Nebraska Research Initiative (NRI) and NIH awards.

Conflicts of Interest: The authors declare that they have no conflicts of interest.

References

1. Hickman, D.L.; Johnson, J.; Vemulapalli, T.H.; Crisler, J.R.; Shepherd, R. Commonly Used Animal Models. In *Principles of Animal Research for Graduate and Undergraduate Students*; 2017.
2. Vandamme, T. Use of Rodents as Models of Human Diseases. *J Pharm Bioallied Sci* 2014, *6*.
3. Nelson, D.R.; Zeldin, D.C.; Hoffman, S.M.G.; Maltais, L.J.; Wain, H.M.; Nebert, D.W. Comparison of Cytochrome P450 (CYP) Genes from the Mouse and Human Genomes, Including Nomenclature Recommendations for Genes, Pseudogenes and Alternative-Splice Variants. *Pharmacogenetics* 2004, *14*.
4. Junhee Seok; H. Shaw Warren; Alex, G.C.; Michael, N.M.; Henry, V.B.; Xu, W.; Richards, D.R.; McDonald-Smith, G.P.; Gao, H.; Hennessy, L.; et al. Genomic Responses in Mouse Models Poorly Mimic Human Inflammatory Diseases. *Proc Natl Acad Sci U S A* **2013**, *110*, doi:10.1073/pnas.1222878110.
5. Bailey, K.L.; Cartwright, S.B.; Patel, N.S.; Remmers, N.; Lazenby, A.J.; Hollingsworth, M.A.; Carlson, M.A. Porcine Pancreatic Ductal Epithelial Cells Transformed with KRASG12D and SV40T Are Tumorigenic. *Sci Rep* **2021**, *11*, doi:10.1038/s41598-021-92852-2.
6. Bailey, K.L.; Carlson, M.A. Porcine Models of Pancreatic Cancer. *Front Oncol* 2019, *9*.
7. Mondal, P.; Bailey, K.L.; Cartwright, S.B.; Band, V.; Carlson, M.A. Large Animal Models of Breast Cancer. *Front Oncol* 2022, *12*.
8. Mondal, P.; Patel, N.S.; Bailey, K.; Aravind, S.; Cartwright, S.B.; Hollingsworth, M.A.; Lazenby, A.J.; Carlson, M.A. Induction of Pancreatic Neoplasia in the KRAS/TP53 Oncopig. *Dis Model Mech* **2023**, *16*, doi:10.1242/dmm.049699.
9. Wernersson, R.; Schierup, M.H.; Jørgensen, F.G.; Gorodkin, J.; Panitz, F.; Stærfeldt, H.H.; Christensen, O.F.; Mailund, T.; Hornshøj, H.; Klein, A.; et al. Pigs in Sequence Space: A 0.66X Coverage Pig Genome Survey Based on Shotgun Sequencing. *BMC Genomics* **2005**, *6*, doi:10.1186/1471-2164-6-70.

10. Groenen, M.A.M.; Archibald, A.L.; Uenishi, H.; Tuggle, C.K.; Takeuchi, Y.; Rothschild, M.F.; Rogel-Gaillard, C.; Park, C.; Milan, D.; Megens, H.J.; et al. Analyses of Pig Genomes Provide Insight into Porcine Demography and Evolution. *Nature* **2012**, *491*, doi:10.1038/nature11622.
11. Schook, L.B.; Collares, T. V.; Darfour-Oduro, K.A.; De, A.K.; Rund, L.A.; Schachtschneider, K.M.; Seixas, F.K. Unraveling the Swine Genome: Implications for Human Health. *Annu Rev Anim Biosci* **2015**, *3*, doi:10.1146/annurev-animal-022114-110815.
12. Nakamura, T.; Fujiwara, K.; Saitou, M.; Tsukiyama, T. Non-Human Primates as a Model for Human Development. *Stem Cell Reports* 2021, *16*.
13. Yan, G.; Zhang, G.; Fang, X.; Zhang, Y.; Li, C.; Ling, F.; Cooper, D.N.; Li, Q.; Li, Y.; Van Gool, A.J.; et al. Genome Sequencing and Comparison of Two Nonhuman Primate Animal Models, the Cynomolgus and Chinese Rhesus Macaques. *Nat Biotechnol* **2011**, *29*, doi:10.1038/nbt.1992.
14. Matsuzaki, M.; Ebina, T. Common Marmoset as a Model Primate for Study of the Motor Control System. *Curr Opin Neurobiol* 2020, *64*.
15. Howe, K.L.; Achuthan, P.; Allen, J.; Allen, J.; Alvarez-Jarreta, J.; Ridwan Amode, M.; Armean, I.M.; Azov, A.G.; Bennett, R.; Bhai, J.; et al. Ensembl 2021. *Nucleic Acids Res* **2021**, *49*, doi:10.1093/nar/gkaa942.
16. Camacho, C.; Coulouris, G.; Avagyan, V.; Ma, N.; Papadopoulos, J.; Bealer, K.; Madden, T.L. BLAST+: Architecture and Applications. *BMC Bioinformatics* **2009**, *10*, doi:10.1186/1471-2105-10-421.
17. Conway, J.R.; Lex, A.; Gehlenborg, N. UpSetR: An R Package for the Visualization of Intersecting Sets and Their Properties. *Bioinformatics* **2017**, *33*, doi:10.1093/bioinformatics/btx364.
18. Yu, Y.; Ouyang, Y.; Yao, W. ShinyCircos: An R/Shiny Application for Interactive Creation of Circos Plot. *Bioinformatics* **2018**, *34*, doi:10.1093/bioinformatics/btx763.
19. Larkin, M.A.; Blackshields, G.; Brown, N.P.; Chenna, R.; Mcgettigan, P.A.; McWilliam, H.; Valentin, F.; Wallace, I.M.; Wilm, A.; Lopez, R.; et al. Clustal W and Clustal X Version 2.0. *Bioinformatics* **2007**, *23*, doi:10.1093/bioinformatics/btm404.
20. Page, A.J.; Taylor, B.; Delaney, A.J.; Soares, J.; Seemann, T.; Keane, J.A.; Harris, S.R. SNP-Sites: Rapid Efficient Extraction of SNPs from Multi-FASTA Alignments. *Microb Genom* **2016**, *2*, doi:10.1099/mgen.0.000056.
21. McLaren, W.; Gil, L.; Hunt, S.E.; Riat, H.S.; Ritchie, G.R.S.; Thormann, A.; Flicek, P.; Cunningham, F. The Ensembl Variant Effect Predictor. *Genome Biol* **2016**, *17*, doi:10.1186/s13059-016-0974-4.
22. Oscanoa, J.; Sivapalan, L.; Gadaleta, E.; Dayem Ullah, A.Z.; Lemoine, N.R.; Chelala, C. SNPnexus: A Web Server for Functional Annotation of Human Genome Sequence Variation (2020 Update). *Nucleic Acids Res* **2020**, *48*, doi:10.1093/NAR/GKAA420.
23. Piñero, J.; Ramírez-Anguita, J.M.; Saüch-Pitarch, J.; Ronzano, F.; Centeno, E.; Sanz, F.; Furlong, L.I. The DisGeNET Knowledge Platform for Disease Genomics: 2019 Update. *Nucleic Acids Res* **2020**, *48*, doi:10.1093/nar/gkz1021.
24. Gel, B.; Serra, E. KaryoploteR: An R/Bioconductor Package to Plot Customizable Genomes Displaying Arbitrary Data. *Bioinformatics* **2017**, *33*, doi:10.1093/bioinformatics/btx346.
25. Rice, P.; Longden, L.; Bleasby, A. EMBOSS: The European Molecular Biology Open Software Suite. *Trends in Genetics* 2000, *16*.
26. Price, M.N.; Dehal, P.S.; Arkin, A.P. FastTree 2 - Approximately Maximum-Likelihood Trees for Large Alignments. *PLoS One* **2010**, *5*, doi:10.1371/journal.pone.0009490.
27. Tamura, K.; Stecher, G.; Kumar, S. MEGA11: Molecular Evolutionary Genetics Analysis Version 11. *Mol Biol Evol* **2021**, *38*, doi:10.1093/molbev/msab120.
28. Papatheodorou, I.; Fonseca, N.A.; Keays, M.; Tang, Y.A.; Barrera, E.; Bazant, W.; Burke, M.; Füllgrabe, A.; Fuentes, A.M.P.; George, N.; et al. Expression Atlas: Gene and Protein Expression across Multiple Studies and Organisms. *Nucleic Acids Res* **2018**, *46*, doi:10.1093/nar/gkx1158.
29. Wei, T.; Simko, V. Corrplot: Visualization of a Correlation Matrix. R Package Version 0.84. Https://Github.Com/Taiyun/Corrplot. *Statistician* 2017, *56*.
30. Harding, J.D. Nonhuman Primates and Translational Research: Progress, Opportunities, and Challenges. *ILAR J* **2017**, *58*, doi:10.1093/ilar/ilx033.
31. Feng, G.; Jensen, F.E.; Greely, H.T.; Okano, H.; Treue, S.; Roberts, A.C.; Fox, J.G.; Caddick, S.; Poo, M.M.; Newsome, W.T.; et al. Opportunities and Limitations of Genetically Modified Nonhuman Primate Models for Neuroscience Research. *Proc Natl Acad Sci U S A* 2020, *117*.
32. Miller, C.T.; Freiwald, W.A.; Leopold, D.A.; Mitchell, J.F.; Silva, A.C.; Wang, X. Marmosets: A Neuroscientific Model of Human Social Behavior. *Neuron* 2016, *90*.
33. Pomberger, T.; Risueno-Segovia, C.; Gultekin, Y.B.; Dohmen, D.; Hage, S.R. Cognitive Control of Complex Motor Behavior in Marmoset Monkeys. *Nat Commun* **2019**, *10*, doi:10.1038/s41467-019-11714-8.
34. Ludlage, E.; Mansfield, K. Clinical Care and Diseases of the Common Marmoset (Callithrix Jacchus). In Proceedings of the Comparative Medicine; 2003; Vol. 53.

35. David, J.M.; Dick, E.J.; Hubbard, G.B. Spontaneous Pathology of the Common Marmoset (Callithrix Jacchus) and Tamarins (Saguinus Oedipus, Saguinus Mystax). *J Med Primatol* **2009**, *38*, doi:10.1111/j.1600-0684.2009.00362.x.
36. Conley, A.J.; Moeller, B.C.; Nguyen, A.D.; Stanley, S.D.; Plant, T.M.; Abbott, D.H. Defining Adrenarche in the Rhesus Macaque (Macaca Mulatta), a Non-Human Primate Model for Adrenal Androgen Secretion. *Mol Cell Endocrinol* 2011, *336*.
37. Higham, J.P.; Heistermann, M.; Maestripieri, D. The Endocrinology of Male Rhesus Macaque Social and Reproductive Status: A Test of the Challenge and Social Stress Hypotheses. *Behav Ecol Sociobiol* **2013**, *67*, doi:10.1007/s00265-012-1420-6.
38. Litten-Brown, J.C.; Corson, A.M.; Clarke, L. Porcine Models for the Metabolic Syndrome, Digestive and Bone Disorders: A General Overview. *Animal* **2010**, *4*, doi:10.1017/S1751731110000200.
39. Koopmans, S.J.; Schuurman, T. Considerations on Pig Models for Appetite, Metabolic Syndrome and Obese Type 2 Diabetes: From Food Intake to Metabolic Disease. *Eur J Pharmacol* 2015, *759*.
40. Morey-Holton, E.R.; Globus, R.K. Hindlimb Unloading Rodent Model: Technical Aspects. *J Appl Physiol* 2002, *92*.
41. Witsø, E.; Hoang, L.; Løseth, K.; Bergh, K. Establishment of an in Vivo Rat Model for Chronic Musculoskeletal Implant Infection. *J Orthop Surg Res* **2020**, *15*, doi:10.1186/s13018-020-1546-6.
42. Grisel, P.; Meinhardt, A.; Lehr, H.A.; Kappenberger, L.; Barrandon, Y.; Vassalli, G. The MRL Mouse Repairs Both Cryogenic and Ischemic Myocardial Infarcts with Scar. *Cardiovascular Pathology* **2008**, *17*, doi:10.1016/j.carpath.2007.01.007.
43. Unsld, B.; Schotola, H.; Jacobshagen, C.; Seidler, T.; Sossalla, S.; Emons, J.; Klede, S.; Knll, R.; Guan, K.; El-Armouche, A.; et al. Age-Dependent Changes in Contractile Function and Passive Elastic Properties of Myocardium from Mice Lacking Muscle LIM Protein (MLP). *Eur J Heart Fail* **2012**, *14*, doi:10.1093/eurjhf/hfs020.
44. Sarkar, S.; Chawla-Sarkar, M.; Young, D.; Nishiyama, K.; Rayborn, M.E.; Hollyfield, J.G.; Sen, S. Myocardial Cell Death and Regeneration during Progression of Cardiac Hypertrophy to Heart Failure. *Journal of Biological Chemistry* **2004**, *279*, doi:10.1074/jbc.M402037200.
45. Elliott, J.F.; Liu, J.; Yuan, Z.N.; Bautista-Lopez, N.; Wallbank, S.L.; Suzuki, K.; Rayner, D.; Nation, P.; Robertson, M.A.; Liu, G.; et al. Autoimmune Cardiomyopathy and Heart Block Develop Spontaneously in HLA-DQ8 Transgenic IAβ Knockout NOD Mice. *Proc Natl Acad Sci U S A* **2003**, *100*, doi:10.1073/pnas.2235552100.
46. Xu, Y.; Wu, Z.; Liu, L.; Liu, J.; Wang, Y. Rat Model of Cockayne Syndrome Neurological Disease. *Cell Rep* **2019**, *29*, 800-809.e5, doi:https://doi.org/10.1016/j.celrep.2019.09.028.
47. Harper, A. Mouse Models of Neurological Disorders-A Comparison of Heritable and Acquired Traits. *Biochim Biophys Acta Mol Basis Dis* 2010, *1802*.
48. Hutter, C.; Zenklusen, J.C. The Cancer Genome Atlas: Creating Lasting Value beyond Its Data. *Cell* 2018, *173*.